JOURNAL OF Materials CHEMISTRY

Reaction in Al_2O_3 surface layers upon ion implantation

Jun Tian,[a] Qizu Wang,[b] Yufeng Chen[c] and Qunji Xue[a]

[a]*Laboratory of Solid Lubrication, Lanzhou Institute of Chemical Physics, Chinese Academy of Sciences, Lanzhou 730000, China. E-mail: tianjun@public.lz.gs.cn*
[b]*Department of Materials Science, Lanzhou University, Lanzhou 730000, China*
[c]*China Building Materials Academy, Beijing 100024, China*

Received 9th July 1999, Accepted 30th November 1999

The mechanical properties of Al_2O_3 have been improved by implantation of C and N ions at doses of 1×10^{15} to 1×10^{18} ion cm^{-2}. The hardness, fracture and scratch toughness of the implanted layers were examined. The increase in hardness was *ca.* 92% at 1×10^{17} N ions cm^{-2}, but only 6% at 1×10^{17} C ions cm^{-2}. The maximum fracture toughness was 95% greater than that of the unimplanted substrate at a fluence of 3×10^{17} N ions cm^{-2}, and *ca.* 25% greater for 5×10^{17} C ions cm^{-2}. The mechanisms of hardening and toughening by C and N ion implantation were investigated by XPS, electrical resistance and Raman spectroscopy measurements. The surface electric resistivity decreased to *ca.* $10^7\ \Omega$ cm for N^+ or C^+ ion implantation. Nitrogen implantation produced Al, AlN or AlON while carbon implantation led to a carbon film, Al, Al_4C_3 or Al_4O_4C on Al_2O_3. The hardening and toughening on Al_2O_3 surface layers was attributed to chemical reactions, with the amount of modification depending on the C and N ion implantation dose.

Introduction

Alumina, one of the most widely used wear, heat and electrical-resistant materials, has a high hardness and excellent chemical stability even at high temperatures. At high contact stresses significant amounts of cracking can occur around scratches in brittle materials. In this case, there are large oscillations in the friction trace and much of the frictional energy is dissipated in fracture processes. Previous work indicates that the friction coefficients and the wear rates of the most commonly used ceramics are unacceptably high under 'dry' conditions. Effort has been devoted very recently to surface modification of ceramics. Since the early 1980s, there have been a number of studies of the effect of implantation on the surface mechanical properties of ceramics.[1,2] Surface modification by energetic particles leads to surface damage, even though a new functional layer is generated on the materials with improved physical and chemical properties, such as adhesion, surface hardness, corrosion resistance and wear resistance. Implantation-induced changes in the surface charge state may also affect the adhesion of lubricant molecules.[3] An increase of mechanical strength by high energy ion implantation has been attributed to compressive surface residual stress upon volume expansion in the implanted region by introduction of defects.[4] Such residual stresses should have a marked effect on hardness, fracture toughness and tribological properties.[5] Relevant examples include microtribology between ceramics and metals or diamond-like carbon films or oil on a hard disc or micromachine, lubrication of bearings using ion implanted MoS_2, ceramic motors at high temperatures and bioceramic devices[6] in life. For Al_2O_3 it was reported that the fracture toughness increased by 10–15% and the residual stress by 20–60% upon implanting Ni into Al_2O_3 at 1×10^{15} to 1×10^{17} ions cm^{-2},[7] while the surface of Al_2O_3 was found to be amorphous after a fluence of 1×10^{17} Cr^+ cm^{-2}.[8] The implanted surface was amorphized or damaged by implantation at room temperature by Pt, W, Y ions,[9,10] with the amorphized surface layer being 150 nm thick. It is observed that a thin layer, differing in structure from the bulk is formed at the wear surface of unimplanted oxide ceramics. Once the surface layer is formed, it readily undergoes shear deformation owing to its low deformation resistance. This can be achieved by use of solid-lubricant coatings,[11] self-lubricating ceramic-matrix composites,[12] or reaction of the layer with the environment by implantation (*i.e.* in a gaseous environment rather than a high vacuum).[13–15]

The objective of this study, in which Al_2O_3 was subjected to ion implantation was to investigate the modifications to the mechanical properties and surface structure and to understand the mechanisms of layer reactions which lead to modifications.

Experimental

α-Al_2O_3 single crystals with optical polished surfaces were used as substrates, Al_2O_3 blocks were cut into 15 mm × 1.5 mm strips. To reduce damage induced by the polishing, the samples were post-annealed in air for 15 h at 1200 °C. The samples were cleaned at room temperature in acetone ultrasonic baths, then implanted with N and C ions with energies of 110 keV. A 0.11 ± 0.02 μm thickness of thin ion-plating Ag film was applied to the Al_2O_3 substrate by N^+ ion implantation.[12] The pressure in the target chamber was *ca.* 4–7 mPa during implantation and the ion dose varied between 1×10^{15} and 1×10^{18} ion cm^{-2}. To avoid heating effects, the samples were clamped onto a water-cooled copper plate, and the ion current densities were kept to 16–20 μA cm^{-2}. Parts of each sample were shielded from the ion bombardment to retain unimplanted areas to allow comparative measurements on the crystal surface of implanted/unimplanted regions.

Both the range and the damage distributions beneath the implanted layer may be approximated by Gaussian profiles. For the implantation used here, the energy loss, the spread of the range and the damage distributions were calculated using the Monte Carlo method TRIM88 and results are presented in Table 1. The electronic energy loss $(dE/dX)_e$ is greater than the nuclear energy loss $(dE/dX)_n$, near the surface. The projected mean ion range is *ca.* 162 nm for N^+ at 110 keV.

Ion implantation of Al_2O_3 should produce compositional microstructural and mechanical changes in the surface and near-surface regions. After implantation, microhardness measurement (by HX-1000) was performed, Vickers microhardness was obtained at a load of 0.24 N. The microhardness was given as a function of the load and penetration depth of the indenter.

Table 1 Range and damage parameters for α-Al_2O_3 implanted by N^+ implantation

Energy loss/keV μm^{-1}					
$(dE/dX)_e$	$(dE/dX)_n$	Projected mean ion range, $R_p/\mu m^{-1}$	Standard deviation, $\Delta R_p/\mu m^{-1}$	Projected mean damage depth, $X_d/\mu m^{-1}$	Standard deviation, $\Delta X_d/\mu m^{-1}$
580.2	107.3	0.16	0.04	0.15	0.04

A method to determine indentation toughness has been described by Lawn and Fuller who related the changes in lengths of radial cracks around an indentation to the state of a thin surface layer. Indentation toughness K_{Ic} at load of 4.90 N was calculated by,[16]

$$K_{Ic} = 0.203(c/a)^{-3/2} H_v a^{1/2}$$

Scratch tests of implanted layers were performed using a WS-91 automatic scratch tester equipped with a 120° diamond indenter with the radius of the indenter vertex being 0.2 mm. The specimen slowly moved, while the load of indenter gradually increased. When the surface layer of the specimen is not broken, the indenter continuously slides on the surface. When the load reaches a critical level, the layer of the specimen is broken, and the output is recorded as scratch noise. A micrograph of the scratch trace was observed by scanning electron microscopy (JEM-1200EX, operating voltage 40 kV, with prior coating by an Au film).

The surface composition was investigated using a PHI-550 model (Mg-Kα) surface analysis system. The ESCA spectrum was obtained after etching with a 3 kV Ar ion gun under a pressure of 1×10^{-5} Pa for 30 s. Raman shift measurements were performed on Al_2O_3 crystals using a SPEX-1403 Raman spectrometer equipped with a 514 nm argon ion laser at a power of 20 mW. The electrical resistivities were measured with a two-point probe apparatus.

Results

The surface mechanical properties of ceramics can be altered by ion implantation. Fig. 1 shows the variation of hardness of an implanted Al_2O_3 single crystal specimen as a function of the dose. The relative hardness is quoted which is the ratio of implanted specimen hardness to that of the unimplanted material. The hardness increases with an increase of fluence and becomes highest at 1×10^{17} ions cm^{-2}. The maximum hardness increase is about 92% for N , but only 6% for C . The hardness then rapidly decreases to 48% or 66% of that of the unimplanted sample using a dose of 3×10^{17} N ions cm^{-2} or 1×10^{18} C ions cm^{-2}, respectively. Ceramics are considered to be brittle and have low toughness because the work required to propagate a crack is less than the work to create the crack. Fig. 2 shows the relative toughness for implanted Al_2O_3. The fracture toughness increases monotonically with an increasing fluence of N implantation. At a fluence of 3×10^{17} N ions cm^{-2}, the fracture toughness is 95% greater than that of the unimplanted substrate while for C the fracture toughness is *ca.* 25% greater for 5×10^{17} C ions cm^{-2}, and then decreases. The critical peeling load of the implanted Al_2O_3 layer shows the same increasing tendency as the toughness

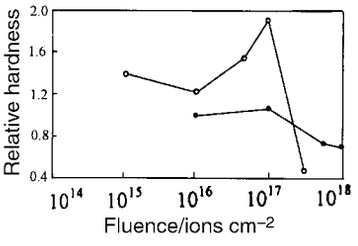

Fig. 1 Relative hardness for implanted Al_2O_3; (○) N ions, (●) C ions.

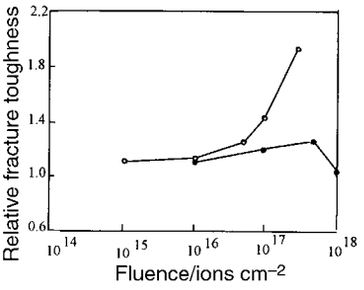

Fig. 2 Relative fracture toughness for implanted Al_2O_3; (○) N ions, (●) C ions.

Table 2 Relative critical peeling load of implantation materials

	Fluence (ions cm^{-2})				
	1×10^{15}	1×10^{16}	1×10^{17}	5×10^{17}	1×10^{18}
N ion implanted Al_2O_3	1	—[a]	1.54	—[a]	—[a]
C ion implanted Al_2O_3	—[a]	1.30	1.30	1.48	1.43
N ion implanted Ag/Al_2O_3	2.75	3.00	3.32	—[a]	—[a]

[a]Not measured.

curves (Table 2), in particular, formation of Ag/Al_2O_3 at the interface gives a high peeling load at low doses.[12] Fig. 3 shows SEM photographs of scratches at the critical load. Indentation of the unimplanted substrate leads to cracks initiating within the substrate and propagating toward the surface, with formation of long lateral crack patterns. The wear debris produced from the unimplanted material is sharp and angular indicating brittle fracture around the scratch [Fig. 3(a)]. The strong dependence of the formation of lateral cracks on the fluence suggests that ion implantation of Al_2O_3 is especially effective for the fracture processes. When the samples are bombarded the size of the cracks are reduced. Cracks were deflected by the N implanted surface layer and thus their extent on the free surface is shorter [Fig. 3(b)]. At an implantation dose of 1×10^{17} N ions cm^{-2} lateral cracks are no longer visible, however, examination of the cracks reveals that the semicircular crack trace becomes oblate for implanted samples [Fig. 3(c)], and the cracks penetrate small distances into the material. This effectively raises the resistance to fracture damage. In C implanted materials, the same result of plasticity around the scratch trace has been reported.[14] It is clear that the properties of the implanted zone affect the crack propagation process and prevent subsurface cracks from reaching the free surface. This should increase the wear resistance as compared to unimplanted materials because of the ion induced enhanced surface layer toughness of Al_2O_3.

The question arises as to whether hardening and toughening for experiments using C and N ion implantation are due to the operation of a radiation-hardening mechanism or some other factor?

Discussion

Fig. 4 shows the high resolution XPS spectra for Al 2p, O 1s, N 1s and C 1s. The Al 2p peak appears at 74.2 and 72.7 eV for 1×10^{17} N ion cm^{-2} and 5×10^{17} C ion cm^{-2} implanted Al_2O_3,

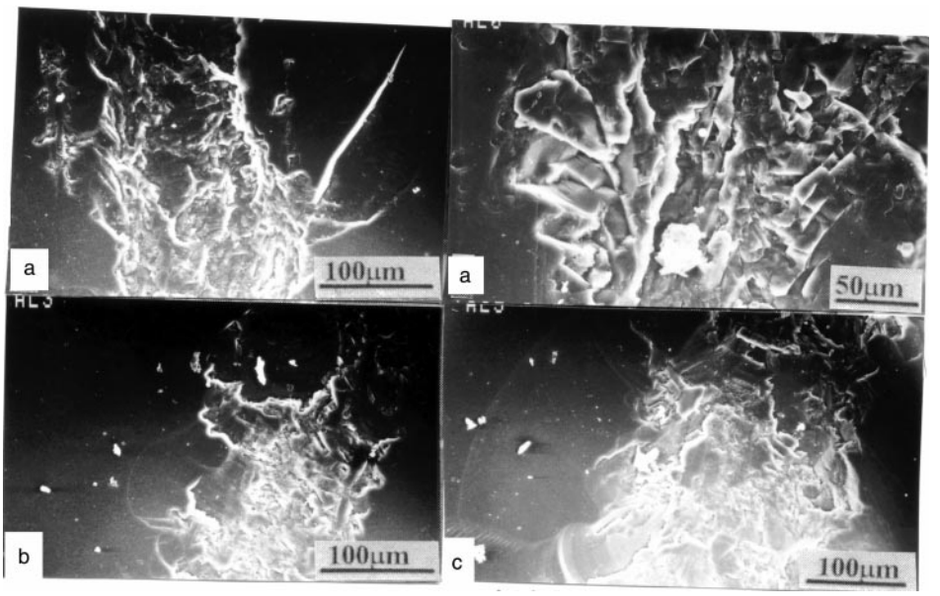

Fig. 3 Scratch photographs of N implanted Al_2O_3; (a) unimplanted (load 11.7 N), (b) 1×10^{15} N^+ cm^{-2} (load 11.7 N), (c) 1×10^{17} N^+ cm^{-2} (load 18.0 N).

respectively. This indicates that elemental Al (72.7 eV) is formed in the surface layer. The N 1s spectrum becomes wider for N^+ implanted Al_2O_3 or Ag/Al_2O_3, and the peak at 397.5 eV is assigned to AlN or AlON.[15,17] Definitive information was

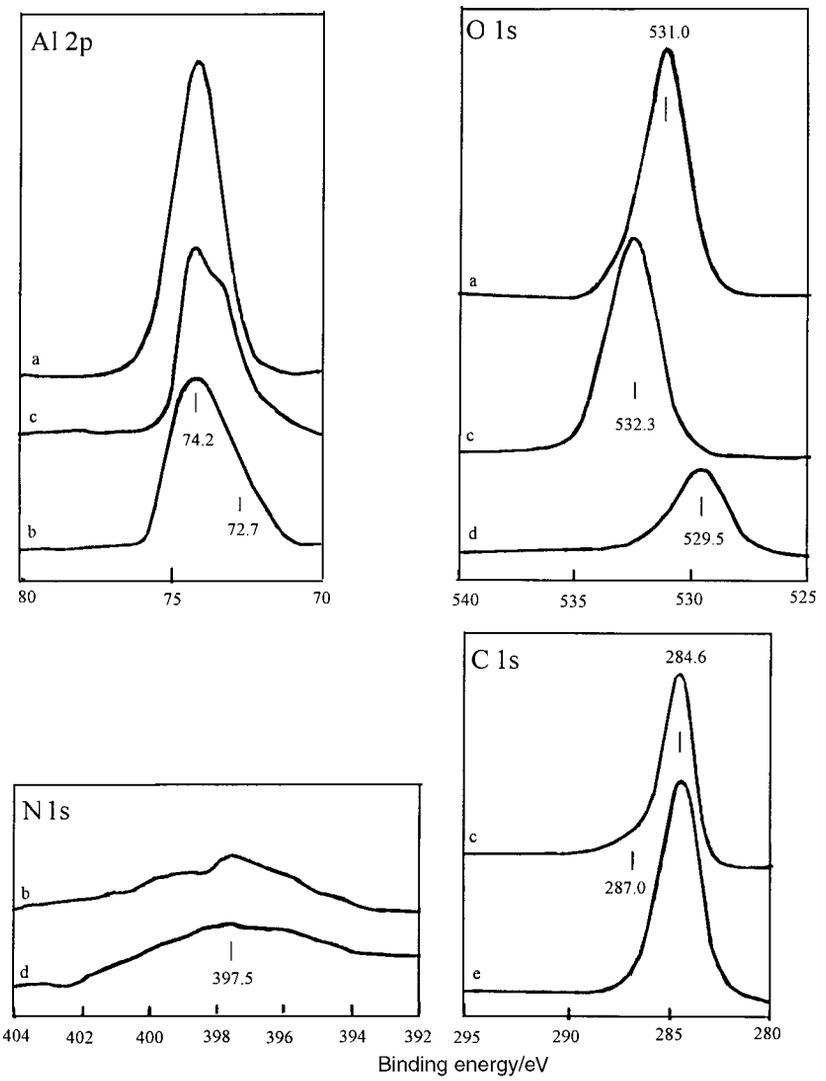

Fig. 4 XPS spectra for (a) Al_2O_3, (b) 1×10^{17} N ion implanted Al_2O_3, (c) 5×10^{17} C ion implanted Al_2O_3, (d) 1×10^{17} N ion implanted Ag/Al_2O_3 and (e) graphite.

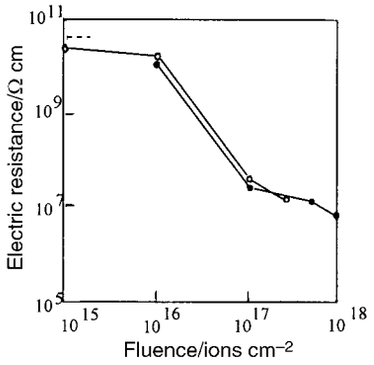

Fig. 5 Surface electrical resistance of implanted Al_2O_3; (○) N ion, (●) C ion, (---) unimplanted.

not obtained from the Al 2p spectrum (74.2 eV) because any signal from AlN or Al_4C_3 was obscured by that from Al_2O_3. The O 1s spectrum (Fig. 4) shows a peak at 529.5 eV which can be attributed to Ag_2O[18] for N^+ implanted Ag/Al_2O_3. The occurrence of an interfacial reaction should improve the adhesion between the metal and the ceramic substrate, as is the case for the formation of $Al_2O_3{\cdot}AlN$ and α-$Ag_2O{\cdot}Al_2O_3$ on Ag/Al_2O_3[12] by N^+ implantation as shown by XRD. Peaks at 532.3 eV (O 1s) and 287.0 eV (C 1s) can be attributed to formation of Al_4O_4C by C^+ implantation. The friction dramatically decreases with increased implantation C dose, owing to a hydrogenated carbon film being formed on the surface.[14,19] It is therefore suggested that the observed reduction in friction is related to the formation of an amorphous and solid lubricant layer upon ion implantation, and that the low friction state is maintained until the surface layer is worn away. The formation of Al, carbon film and AlN (for which the electric resistance is estimated to be $5.6 \times 10^4\ \Omega\ cm$[20]) on the implanted Al_2O_3 surface reduces the surface electric resistivity to *ca.* $10^7\ \Omega$ cm after $1 \times 10^{17}\ N^+$ or C^+ ion cm^{-2} (Fig. 5). The decrease of the surface electrical resistance is not attributable to the formation of an amorphous Al_2O_3 layer at high dose, either by nitrogen or carbon ion implantation, since experimental evidence indicates that new species were formed on the Al_2O_3 surface owing to reactions caused by the implanted ions.

From the above results, we assume that the reaction of implanted Al_2O_3 with nitrogen produces AlN or AlON[21,22] according to eqn. (1).

$$2Al_2O_3 + 7/2N_2{}^+ \rightarrow AlN + 2AlON + Al + 4NO \qquad (1)$$

while the reaction of implanted Al_2O_3 with carbon produces Al and Al_4O_4C or Al_4C_3:[23]

$$8Al_2O_3 + 27C^+ \rightarrow 2Al_4C_3 + Al_4O_4C + 20CO + 4Al \qquad (2)$$

Small bubbles have been observed on C^+ implanted Al_2O_3,[14] and McHargue[24] *et al.* have obtained a similar surface state of implanted sapphire with rare gases (ionized Ar, Ne). Such surface bubbles and cavity formation may be attributed to CO or NO bubble formation in implanted Al_2O_3. Generally, these reactions occur at high temperatures, but the non-equilibrium process of implantation also leads to occurrence of these reactions. In addition, a higher reaction temperature leads to a carbon phase on a C^+ implanted surface according to Raman spectra. The Raman spectrum of large single-crystal graphite shows a single peak at $1580\ cm^{-1}$ while non-crystalline graphite shows a peak at $1560\ cm^{-1}$.[25,26] For amorphous carbon, the absence of long range order leads to a new band at *ca.* $1360\ cm^{-1}$. Studies of graphite materials by Raman spectroscopy show a linear relationship between the intensity ratio $I(1360)/I(1560)$ and the degree of crystallinity. Unimplanted Al_2O_3 shows three distinct Raman peaks at 372, 410 and $638\ cm^{-1}$ with no peaks in the range 1200–1700 cm^{-1} [Fig. 6(a)]. The implanted specimen at $1 \times 10^{17}\ C^+\ cm^{-2}$ dose shows peaks at 1354 and 1556 [Fig. 6(b)]. A low $I(1360)/I(1560)$ ratio for a $1 \times 10^{18}\ C^+\ cm^{-2}$ dose indicates a good graphite structure [Fig. 6(c)] and the C/O atom ratio is 6.7 according ESCA. At the same time, the sample became of a dark appearance when implantation reached 5×10^{17} C ions cm^{-2}. Raman spectroscopy indicated a graphite phase on the surface at high implantation dose, and may explain the high temperature behavior of the surface upon implantation, and explain the low electrical resistance and low friction.

Thus, the observation of greatly different hardening and toughening of Al_2O_3 by C or N ion implantation can be attributed to the surface layer reactions at high dose. For N ion implantation, the hardness increased greatly because of the hard nature of AlN or AlON formed at $1 \times 10^{17}\ N^+\ cm^{-2}$. A rapid decrease in hardness accompanied by a toughness increase at $3 \times 10^{17}\ N^+\ cm^{-2}$ follows because of the generation of an Al and AlN or AlON mixing layer with lower electrical resistance. During carbon implantation, carbon atoms combine to form carbide compounds while at high C concentrations the proportion of C–C bonds increases and results in the outward growth of a hydrogenated carbon film at high implantation doses. Formation of C–C bonds (284.6 eV), Al or Al_4O_4C lowers the electrical resistance and would lead to a decrease in the hardness and toughness at $1 \times 10^{18}\ C^+\ cm^{-2}$. Both chemical reactions and amorphization of the ceramic surface layer at high implantation fluences can be proposed to explain variations on toughness and hardness of the substrate.

Conclusion

It is shown that ion implantation of an Al_2O_3 surface leads to significant modifications of mechanical properties such as hardness, fracture toughness and friction. The properties are very sensitive to the presence of ion species induced by implantation and to modification of the surface composition. The implantation reaction produces Al, AlN or AlON with nitrogen whereas carbon film, Al, Al_4C_3 or Al_4O_4C are

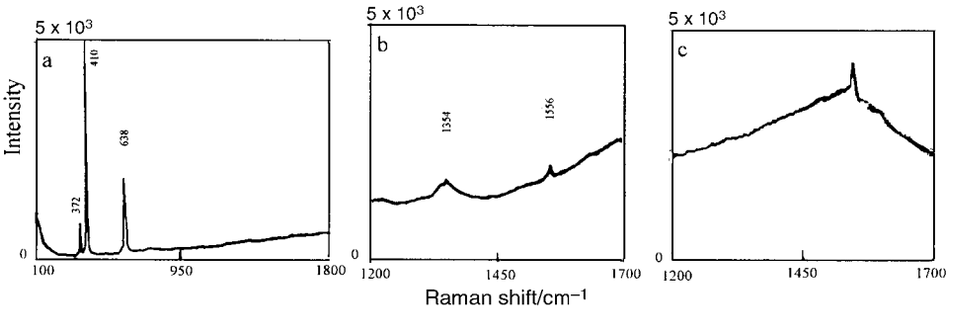

Fig. 6 Raman shift on implanted Al_2O_3 surfaces; (a) unimplanted, (b) $1 \times 10^{17}\ C^+\ cm^{-2}$, (c) $1 \times 10^{18}\ C^+ cm^{-2}$.

obtained with carbon, which lead to different physical properties of the resulting samples. The possibility of forming solid-lubricant films, new self-lubricating ceramic-matrix composites, or other reaction layers (such as nano-films on ceramics for electrical or heat applications or as biomedical devices[27]) using ion implantation at low temperatures is suggested from this work.

Acknowledgements

We thank L. M. Zhao at Lanzhou Institute of Modern Physics for ion implantation studies. We also thank S. K. Qi at Lanzhou Institute of Chemical Physics and G. X. Lan at Nankai University for giving us access to X-ray photoelectron (XPS) and Raman facilities.

References

1 F. Halitim, N. Ikhlef, L. Boudoukha and G. Fantozzi, *J. Phys. D: Appl. Phys.*, 1997, **30**, 330.
2 C. J. McHargue, *Nucl. Instrum. Methods B*, 1987, **19/20**, 797.
3 S. J. Bull and T. F. Page, *J. Phys. D: Appl. Phys.*, 1989, **22**, 941.
4 G. C. Farlow, P. S. Sklad, C. W. White and C. J. McHargue, *J. Mater. Res.*, 1990, **5**, 1502.
5 T. Futagami, Y. Aoki, O. Yoda and S. Nagai, *Nucl. Instrum. Methods B*, 1994, **88**, 261.
6 H. Zreiqat, P. Evans and C. R. Howlett, *J. Biomed. Mater. Res.*, 1999, **44**, 389.
7 T. Hioki, A. Itoh, S. Noda, H. Doi, J. Kawamoto and O. Kamigaito, *Nucl. Instrum. Methods B*, 1985, **7/8**, 521.
8 P. J. Burnett and T. F. Page, *J. Mater. Sci.*, 1984, **19**, 3524.
9 D. Z. Xie, D. Z. Zhu, H. C. Pan, H. J. Xu and Z. X. Ren, *J. Phys. D: Appl. Phys.*, 1998, **31**, 1647.
10 E. Alves, R. C. da Silva, M. F. da Silva and J. C. Soares, *Nucl. Instrum. Methods B*, 1999, **147**, 226.
11 F. Brenscheidt, S. Oswald, A. Mucklich, E. Wieser and W. Moller, *Nucl. Instrum. Methods B*, 1997, **129**, 483.
12 J. Tian, Q. J. Xue, Q. Z. Wang and Y. F. Chen, *J. Mater. Sci.*, 1999, **34**, 4051.
13 W. Fischer, H. Wituschek, G. K. Wolf, H. Ferber, R. Heinze and M. Woydt, *Surf. Coat. Technol.*, 1993, **59**, 249.
14 J. Tian, Q. Z. Wang and Q. J. Xue, *Nucl. Instrum. Methods B*, 1998, **143**, 488.
15 S. K. Koh, Y. B. Son, J. S. Gam, K. S. Han, W. K. Choi and H. J. Jung, *J. Mater. Res.*, 1998, **13**, 2560.
16 B. R. Lawn and E. R. Fuller, *J. Mater. Sci.*, 1984, **19**, 4061.
17 W. K. Choi, S. C. Choi, H. J. Jung, S. K. Koh, D. J. Byun and D. W. Kum, *J. Vac. Sci. Technol. A*, 1998, **16**, 3311.
18 G. Schoen, *Surf. Sci.*, 1973, **35**, 96.
19 J. L. Viviente, A. Garcia, A. Loinaz, F. Alonso and J. I. Onate, *Vacuum*, 1999, **52**, 141.
20 K. Ogata, Y. Andon and E. Kamijo, *Nucl. Instrum. Methods B*, 1989, **39**, 178.
21 Y. Kido, M. Kakeno, K. Yamada, T. Hioki, J. Kawamoto and M.Tada, *J. Phys. D: Appl. Phys.*, 1982, **15**, 2067.
22 N. Lieske and R. Hezel, *J. Appl. Phys.*, 1981, **52**, 5806.
23 A. R. Frank, C. W. Finn and J. F. Elliott, *Metall. Trans. B*, 1989, **20**, 161.
24 C. J. McHargue, G. C. Farlow, M. B. Lewis and J. M. Williams, *Nucl. Instrum. Methods B*, 1987, **19/20**, 809.
25 M. Nakamize, R. Kammereck and P. L. Walker, *Carbon*, 1973, **12**, 259.
26 M. Y. Oshikawa, N. Nagai, M. Mastsuki, H. Fukuda, G. H. Katagiri, I. A. Ishitani and I. N. Agai, *Phys. Rev. B: Condens. Matter*, 1992, **46**, 7169.
27 J. C. Bokros, *Carbon*, 1977, **15**, 355.

Paper a905551g